



Structural Characterization of pre-miRNA 155

Won-Je Kim¹, JiYeon Shin^{1,2}, Kyeongmi Bang^{1,2}, Hyun Kyu Song², and Nak-Kyoon Kim^{1*}

¹Advanced Analysis Center, Korea Institute of Science and Technology, Seoul, Korea

²Division of Life Sciences, Korea University, Seoul, Korea

Received Mar 10, 2016; Revised Apr 12, 2016; Accepted May 2, 2016

Abstract MiRNA-155, upregulated in various cancers, is one of the miRNAs that suppress apoptosis of human cancer. Thus, inhibition of the maturation of miRNA-155 could be an effective way to induce apoptotic cancer cell death. The apical stem-loop of the pre-miRNA-155 has been known as a Dicer binding site for RNA cleavage. Here, to understand the molecular basis of the tertiary interaction between pre-miRNA-155 with Dicer, we characterize the structure of the apical stem-loop of pre-miRNA-155 using NMR spectroscopy. The RNA has a stem-bulge-stem-loop-stem structure, which consists of G-C Watson-Crick and G-U Wobble base pairs. The assignments of imino-protons were further confirmed by 2D ¹⁵N-¹H HSQC NMR spectrum. The NMR parameters obtained in this study can be further used to investigate the tertiary interaction between pre-miRNA-155 and other biomolecules such as protein, nucleic acids, or small chemicals which might be used to control the apoptosis of cancer.

Keywords miRNA, pre-miRNA-155, apoptosis, Dicer, RNA structure, NMR

Introduction

MicroRNA (miRNA) is a single-stranded small non-coding RNA consisting of ~ 22 nucleotides.

MiRNA has been shown to regulate gene expression of plants and animals by degradation of mRNA or by post-transcriptional inhibition of protein synthesis. In nucleus the primary miRNAs (pri-miRNAs), the first precursor of miRNA, are generated by RNA polymerase II, and they are further processed by the RNase III enzyme, Drosha, to produce a shorter stem-loop structured pre-miRNA. Next, the pre-miRNAs are exported into the cytoplasm and processed into double stranded ~ 22 nucleotide miRNAs by another RNase III enzyme, Dicer. The mature miRNAs form a RNA-protein complex, called RISC, and negatively regulate their target genes. When the complementary sequence of the miRNA matches perfectly with the target mRNA sequence, mRNA is degraded. However, in the case of imperfect complementary binding of miRNA to mRNA results in translational repression.¹

Recent studies have shown that there are miRNAs correlated with various human cancers. MiRNA-155 has shown to be upregulated in various cancers, and blocks the apoptosis of human cancer.²

Therefore, inhibition of the production of mature miRNA-155 would be an effective way to suppress cancer cell growth. We previously have shown that a short synthetic polypeptide (16 amino acids) bound to pre-miRNA-155, inhibited the generation of mature miRNA-155, and eventually induced apoptotic cancer cell death.³ Since the polypeptide

* Address correspondence to: **Nak-Kyoon Kim**, Advanced Analysis Center, Korea Institute of Science and Technology, Seoul, Korea, Tel: 82-2-958-5996; E-mail: nkkim@kist.re.kr

bound to the apical stem-loop of the pre-miRNA, the Dicer binding site at pre-miRNA-155 was blocked and the generation of mature miRNA-155 was inhibited.

Here, to provide further structural information of pre-miRNA155, we characterized the secondary structure of 38-nucleotide long apical stem-loop part of pre-miRNA-155 by NMR spectroscopy. The base-pairs and the H-bonding, the building block of the RNA structure are determined.

Experimental Methods

RNA synthesis and purification The RNA NMR samples were prepared as described elsewhere.^{4,5} Briefly, the DNA template was chemically synthesized by IDT and purified using 15% denaturing PAGE. The purified DNA was cut from the gel and electro-eluted using Elutrap (Whatman). The residual EDTA from electrophoresis was removed by buffer exchange to water using Amicon filtration system (GE healthcare). Non-labeled RNA was synthesized *in vitro* by mixing rATP, rUTP, rGTP, and rCTP (Sigma Aldrich and GE healthcare) in the transcription buffer with 25mM MgCl₂, T7 RNA polymerase (P266L mutant)⁶, and the purified DNA template with complementary 18 mer DNA promoter sequence. The AU or GC base specific 13C, 15N- labeled RNAs were also synthesized *in vitro* by using 13C, 15N- double labeled rNTPs (Silantes, Inc) and non-labeled rNTPs. The reaction mixtures were incubated in a water bath at 37 °C for 6 - 8 hours, and purified using 15% denaturing gel as described above. For NMR experiments, the purified RNA samples were heated to 95 °C under a dilute condition, immediately cooled on ice, and concentrated to 1 – 1.5 mM. The NMR buffer contains 10mM sodium phosphate (pH7.4) with 10% D₂O.

NMR spectroscopy and analysis NMR spectra were measured on Agilent 600MHz NMR with a z-gradient triple resonance probe at KIST or Bruker 800 MHz and 900 MHz NMR with z-gradient triple resonance cryogenic probe at KBSI, at 10 – 20 °C.

The exchangeable imino protons were identified using 1D 1Hecho proton spectra, and further assigned from 2D ¹H-¹H NOESY and 2D ¹⁵N-¹H HSQC, and 2D HNN COSY NMR spectra. NMR spectra were process using VnmrJ3.2 (Agilent Technologies) and Topspin 3.1 (Bruker), and analyzed using Sparky 3.115 (University of California, San Francisco, CA, USA)

Results

Since the Dicer binding site of the pre-miRNA-155 is located at the apical stem-loop region, our pre-miRNA-155 construct is a truncated form from a full length of pre-miRNA-155 sequence (70 nucleotides) (Figure 1).

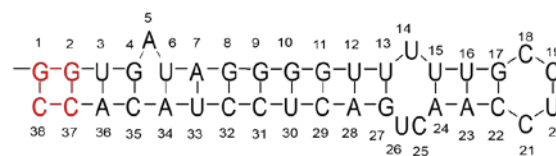


Figure 1. Secondary structure of the apical stem-loop of pre-mi-RNA. The first two GC pairs (red) are artificially added for efficient transcription yield.

Two G-C base pairs at the terminus of RNA are added in order for efficient transcription. The secondary structure predicted from Mfold⁷ showed a stem-bulge-stem-internal loop hairpin structure with a CCUC tetraloop. To confirm whether the predicted secondary structure of the pre-miRNA-155 is correct or not, we first measured the imino proton resonances in the 1D proton spectrum (Figure 2).

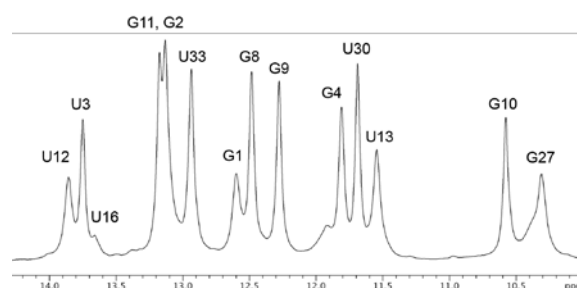


Figure 2. 1D proton NMR spectrum of imino protons.

In the Mfold- predicted RNA structure, there are 15 base pairs, where there are 9 Gs and 8 Us. In each base pair H1 of G or H3 of U will appear in the imino proton resonance region (10 – 15 ppm), so ideally there are maximum of 17 imino protons in the 1D NMR spectrum. There are ~ 14 distinctive imino proton resonances observed in the 1D spectrum, suggesting that the base pairs in the predicted RNA secondary structure is likely to be correct, given that the imino protons at the terminus of each short stem disconnected by a bulge or a loop are not usually observed due to the less protection of H-bonded imino protons from exchange with water protons. To assign each imino proton of pre-miRNA-155, we observed the sequential connectivity between the neighboring imino protons in 2D 1H-1H NOESY spectra (Figure 3).

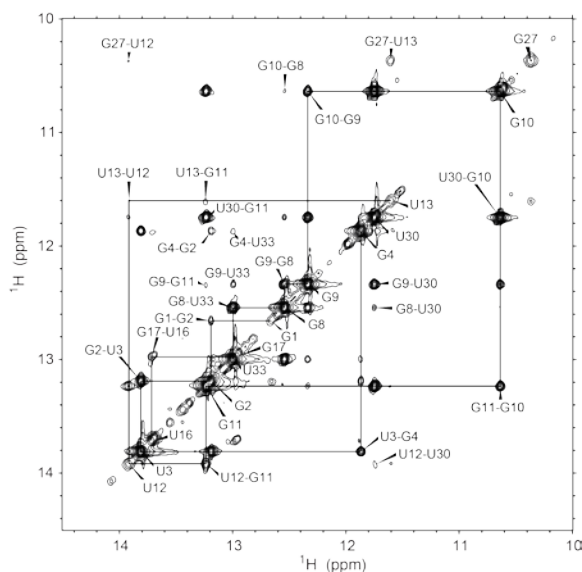


Figure 3. 2D NOESY NMR spectrum of imino protons with 300 ms mixing time at 10 °C.

Since the distance between the neighboring imino protons in the helical region of RNA is about 4 – 5 Å, their NOEs are usually observed if the base pairs are continued. The imino protons of U and G were differentiated in 2D ^{15}N - ^1H HSQC spectra (Figure 4) using AU-specific and GC-specific ^{13}C - ^{15}N -labeled RNAs, respectively, where the imino nitrogen atoms of G and U resonate between 140 – 148 ppm

and between 158 - 165 ppm, respectively.

The base pairs are generated from the canonical Watson-Crick base pairs or other non-canonical base pairs such as Wobble or Hoogsteen base pairs. In

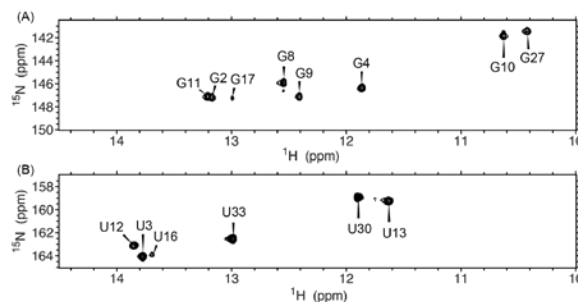


Figure 4. 2D ^{15}N - ^1H HSQC NMR spectra.

Watson-Crick base pairs, H3 of U and H1 of G form H-bonding with their complementary N1 of A and N3 of C, respectively. For GU Wobble base pair, H1 of G forms a H-bonding with O2 of U, and H3 of U with O6 of G. In this case, both imino protons from G and U appear in the NMR spectra. Especially in 2D NOESY spectra, the NOE between these two imino protons are usually observed to be stronger than other NOEs due to the very close proximity between these two protons ($d_{\text{GH1-UH3}} \sim 3 \text{ \AA}$). As predicted in Mfold structure, there are two GU wobble base pairs, G10-U30 and U13-G27, were observed in pre-miRNA-155. The G10-U30 base pair is in the middle of the stem of the A-form helix RNA, so a strong NOE between the two imino protons from GH1 and UH3 are observed. However, for the U13-G27 base pair located at the terminal of the stem, their inter-imino NOE is much less.

In pre-miRNA-155, the sequential connectivity from G1H1 to G4H1 are observed, but the NOE between G4H1 and U6H3 are not observed, implying that the base of bulge A4 is flipped in between the base pairs of G4-C35 and U6-A34. The sequential connectivity resumed from A7-U33 base pair up to U13-G27 base pair. Although the signal of the U16 and G17 imino protons are weak in 1D NMR spectrum, the NOE between the imino protons for U16 and G17 are observed, indicating that the short stem next to the CCUC tetraloop is also formed.

The 2D HNN COSY experiment provides a direct

evidence of the H-bonding in RNA molecules. In this experiment, the H-bonded proton is initially radiated, and the magnetization is transferred to the H-bonded nitrogen of the complementary nucleotide.⁸

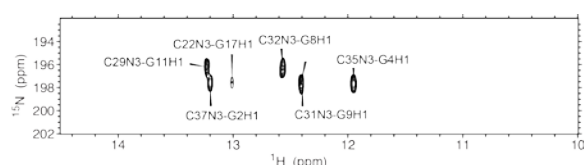


Figure 4. 2D HNN COSY NMR spectrum of pre-miRNA-155.

In the 2D HNN COSY spectra of pre-miRNA-155, only Watson-Crick base pairs are observed in ~ 200 ppm region of f1(15N), where the spectra shows the correlation between the imino protons of Gs and the

N3s of their complementary Cs (Figure 5). Since the H-bonding in the GU wobble base pair is not an N-H...N type, no crosspeak for GU wobble base pair is observed in 2D HNN COSY spectrum. Therefore, this experiment is very useful method for assignment of the base-pairings in the RNA helix.

Conclusion

We determine the secondary structure of the truncated pre-miRNA-155 construct. As predicted in Mfold software, pre-miRNA-155 is composed of three stems composed of 15 base pairs including two GU wobble pairs, a bulge of A4, an internal loop and the CCUC tetraloop.

Acknowledgements

This work was supported by grants from the Basic Science Research Program (NRF-2015R1A2A2A04005596) through the National Research Foundation of Korea, funded by the Ministry of Education, Science, and Technology, and KIST (2V04611).

References

1. M. Ha and V. N. Kim, *Nat. Rev. Mol. Cell Biol.* **15**, 509 (2014)
2. A. Esquela-Kerscher and F. J. Slack, *Nat. Rev. Cancer* **6**, 259 (2006)
3. J. Pai, S. Hyun, J. Y. Hyun, S. H. Park, W.-J. Kim, S. H. Bae, N.-K. Kim, J. Yu, and I. Shin, *J. Am. Chem. Soc.*, **138**, 857 (2016)
4. N.-K. Kim, Y.-S. Nam, and K.-B. Lee, *J. Kor. Mag. Reson. Soc.* **18**, 5 (2014)
5. W.-J. Lee and N.-K. Kim, *J. Kor. Mag. Reson. Soc.* **19**, 143 (2015)
6. J. Gullerez, P.J. Lopez, F. Proux, H. Launay, and M. Dreyfus, *Proc. Natl. Acad. Sci. U.S.A.* **102**, 5958 (2005)
7. M. Zuker, *Nucleic Acids Res.* **31**, 3406 (2003)
8. A. J. Dingley and S. Grzesiek, *J. Am. Chem. Soc.* **120**, 8293 (1998)